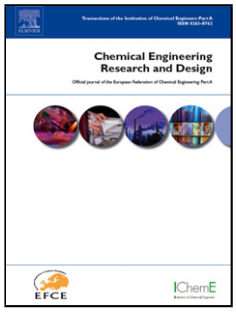

Title: Population balance modelling of stem cell culture in 3D suspension bioreactors

Author: Edoardo Bartolini Harry Manoli Eleonora Costamagna Hari Athitha Jeyaseelan Mouna Hamad Mohammad R. Irhimeh Ali Khademhosseini Ali Abbas

PII: S0263-8762(15)00259-2
DOI: http://dx.doi.org/doi:10.1016/j.cherd.2015.07.014
Reference: CHERD 1964

To appear in:

Received date: 24-6-2015
Revised date: 13-7-2015
Accepted date: 15-7-2015

Please cite this article as: <doi>http://dx.doi.org/10.1016/j.cherd.2015.07.014</doi>

Highlights:

- Mathematical model developed for ESC 3D suspension culture
- Modelled effects of varying substrate and gas concentration on total cell number
- Model behaviour shown to be consistent with literature data
- High initial substrate, O_2, fed-batch system maximise total cell number
- Proof-of-concept model for optimization of stem cell culture in 3D

Population balance modelling of stem cell culture in 3D suspension bioreactors[#]

Edoardo Bartolini[a], Harry Manoli[a], Eleonora Costamagna[a], Hari Athitha Jeyaseelan[a], Mouna Hamad[a], Mohammad R. Irhimeh[b,c], Ali Khademhosseini[d,e,f], Ali Abbas[a]*

[a] *School of Chemical and Biomolecular Engineering, University of Sydney, Sydney NSW 2006, Australia*

[b] *Faculty of Medicine, Dentistry and Health Sciences, University of Western Australia, Crawely, Perth WA 6009, Australia*

[c] *Cell & Tissue Therapies WA, Royal Perth Hospital, Perth WA 6000, Australia*

[d] *Wyss Institute for Biologically Inspired Engineering, Harvard University, Boston, MA 02115, USA*

[e] *Center for Biomedical Engineering, Department of Medicine, Brigham and Women's Hospital, Harvard Medical School, Boston, MA 02139, USA*

[f] *Harvard-MIT Division of Health Sciences and Technology, Massachusetts Institute of Technology, Cambridge MA 02139, USA*

Abstract

Growing and culturing stem cells in scalable quantities is of significant interest for both research and therapy. In this paper, a computational population balance model is developed and validated for the description of specified inter/intra-cellular related stem cell properties of interest (e.g. cell number, mass, size, age). The model describes the effects of extra-cellular variables; (A) bioreactor batch mode initial concentrations (substrate (1.5-5 g/L), dissolved oxygen (hypoxic (5%), normoxic (21%), and hyperoxic (21%)), (B) inoculum (3.75×10^4-5.0×10^5 cells/ml), and (C) fed-batch mode conditions (media feed rate (10-100 ml/h) and air inlet flow rate 0.5-5 l/min). The highest cell concentration achieved within the analysed simulation variable ranges is found to be approximately 1.9x106 cells/ml. Importantly, the results imply the existence of an optimum (maximum) cell

concentration within the extra-cellular variable space, and identifying such optimality is non-trivial and would require a computational optimisation approach for this stem cell bioreactor process.

Keywords: Stem cells; bioreactor; population balance; mathematical modelling.

* *Corresponding Author*: A. Abbas; T: +61 2 9351 3002; F: +61 2 9351 2854; E: ali.abbas@sydney.edu.au

This manuscript is an extension of a paper first presented at the CHEMECA 2014 conference [42].

1. Introduction

Stem cells are a distinctive class of cells in that they are unspecialized and can self-renew [1]. Embryonic stem cells (ESCs) are extracted from the inner cell mass of the developing mammalian blastocyst [2] and are pluripotent, meaning they are characterized by their infinite capability to self-renew while maintaining their aptitude to differentiate into all three primary germ layer cell lineages [2, 3]. As such, they have attracted a great interest in research, biomedicine, and therapy with extensive use in regenerative medicine [4], bone defects [5], retinal degenerative diseases [6], Parkinson's and Huntington's disease [7] and many more [8, 9]. Nevertheless, the most critical problem is the shortage in the stem cell supply and their limited availability due to strict ethics and policies governing their availability and usage. Our aim is to therefore develop an innovative approach for the expansion of stem cells into maximum numbers in minimum time.

The majority of cell-based work in the literature is dominated by cell cultivation on flat 2D surfaces (e.g. T-flasks, well plates) in static conditions [2, 10]. Despite the fact that these methods are straightforward, simple to handle, and of low economical costs, their major drawbacks however are that gas exchange is only permissible at the medium surface, and concentration gradients are very likely to occur within the cell medium itself. Therefore, it is impractical to control parameters such as oxygen or carbon dioxide levels or pH [10, 11]. Three-dimensional (3D) apparatus allow for an increased surface area for the cells to grow in and more strongly resemble the *in vivo* environment of cells. These so called '3D' systems include either a scaffold, which provides a template for cellular growth and/or differentiation, and/or a bioreactor vessel; both systems are effective modes

of culturing and have several key advantages. The latter includes achievable high cell densities, ease of scale-up and control, homogeneity, particularly with respect to oxygen distribution, and other benefits [12-14]. In this paper the term '3D' is used in the biological context, i.e. to refer to the spatial interaction of the cells suspended in the 3D bioreactor environment, and does not refer to computational modelling of the 3D spatial bioreactor space as is traditionally known in the Chemical Engineering modelling context.

The current study presents a detailed mathematical model of stem cell population growth in 3D suspension culture as a first step towards our aim of maximizing cell number and minimizing culture time. The model describes the temporal evolution of stem cell concentration, substrate depletion, dissolved O_2 and CO_2, and metabolite concentrations, simultaneously. From this, variables influencing stem cell growth can be determined, and conditions required for optimal 3D culture can be examined. The model presented in this paper incorporates a population balance model (PBM) [15], oxygen and CO_2 mass transfer dynamics [16], cell death kinetics [17] and equilibrium dynamics from the $CO_2 \leftrightarrow H_2CO_3$ equilibrium occurring due to dissolution of CO_2 is in the growth medium [18]. The model comprising a set of integro-differential-algebraic equations reproduces the three main phases of stem cell growth: exponential phase, stationary phase and death phase (Figure 1). A parameter estimation activity is carried out using the developed model and experimental literature data. A simulation study is then conducted to analyze the effects of variation in above-mentioned process conditions on total stem cell concentration, as well as on the uptake and release of substrates and metabolites.

The next section describes the development of the model and presents the model equations. A comprehensive analysis of the model parameters and model validation are presented in Section 3. Section 4 presents the simulation analysis including results and discussion on the effects of the key variables on the cell population and process behaviours. The paper finishes with conclusions and prospects for the application of this model in optimizing the stem cell culturing process.

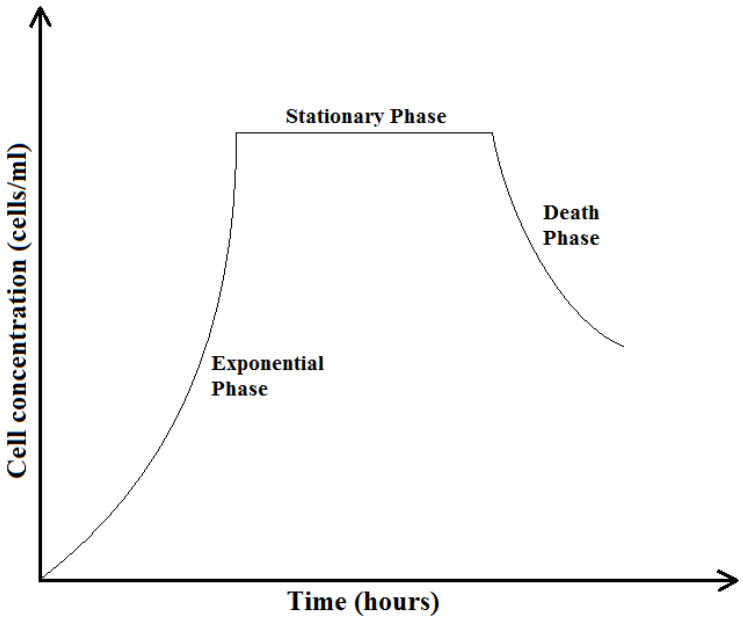

Figure 1 - Illustration of the three main phases of cells growth over time: exponential phase, stationary phase and death phase.

2. Mathematical Modelling

The model herein can be applied to stem cells cultured in a fed-batch stirred suspension bioreactor. While agitation can cause physiological damage to the cells, it is however essential within *in vitro* culture systems to ensure cells are exposed to a homogeneous environment. It is also important to control several other parameters such as nutrients and gas concentrations. At this stage, glucose, as a carbon source, and dissolved O_2 have been considered in particular since they primarily influence stem cell expansion. Waste by-products were also taken into account since their accumulation can initiate cell death, most importantly dissolved CO_2, as it is produced during the process of glucose oxidation. Temperature is kept constant at 37°C and pH constant at 7.4 [19]. Furthermore, this model represents three compartments within the bioreactor: the fermentation broth, the homogeneously dispersed gas bubbles in the broth, and the gas phase above the broth (headspace) (Figure 2).

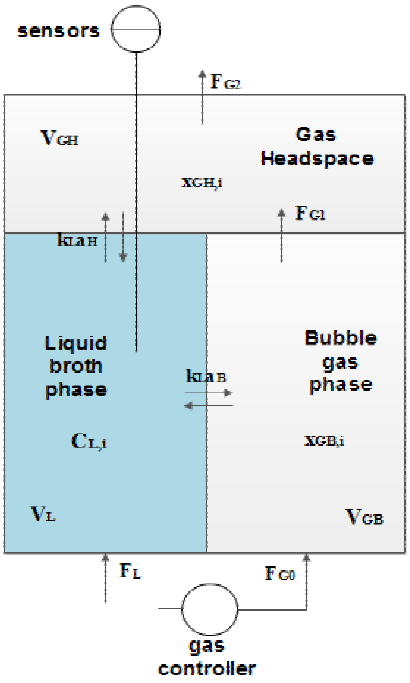

Figure 2 - Illustration of the main compartments of the bioreactor system represented by the model: the bioreactor broth (liquid broth phase), the homogeneously dispersed gas bubbles in the broth (bubble gas phase), and the gas above the broth (gas headspace); i = O_2, CO_2, N_2.

2.1 Population Balance Model

Because an individual cell can be treated as a single particle, this population balance approach traditionally applied to particulate systems is shown in this paper to suit stem cell populations. The population balance model (PBM) is a mathematical formulation of the cell population using cell mass and time as independent variables to take into account both the temporal dynamics of the population, as well as the mass distribution of the cell population.

A generalized form of the population balance of cells in a working 3D culture volume can be described by:

$$\begin{aligned} &Rate\ of\ cell\ accumulation \\ &\quad = rate\ of\ cell\ birth + growth\ flux\ in - growth\ flux\ out \\ &\quad - rate\ of\ cell\ division - rate\ of\ cell\ death \end{aligned} \tag{1}$$

The PBM developed and presented in this paper is based on the works of Eakman [20], Mancuso *et al.* [21, 22], Fredrickson *et al.* [23], Ramakrishna [15], Hjorsto [24], Hatzis and Srienc [25], and

Mantzaris *et al.* [26]. The population balance equation (PBE) presented below is based on assumptions of a well-agitated bioreactor:

$$\frac{\partial \psi(m,t)}{\partial t} + \frac{\partial [v\,\psi(m,t)]}{\partial m} = 2\int_{m}^{\infty} \psi(m',t)\,\Gamma^{M}\left(m', C_{L,O_2}\right) p(m,m')\,dm' - \psi(m,t)\,\Gamma^{M}\left(m, C_{L,O_2}\right) - k_D \psi(m,t) \quad (2)$$

With boundary and initial conditions:

$\psi(m,t) = \psi^0(m)\ for\ t = 0\ and\ \forall m$

$\psi(m,t) = 0\ for\ t \geq 0\ and\ m = 0.$

The right hand side boundary condition for Eq. 2 is equal to zero, while the initial condition $\psi^0(m)$ used to solve Eq. 2 is described by an initial cell distribution given by the lognormal distribution:

$$\psi_i(t) = \psi_i^0 = \frac{N_0}{V} \cdot \frac{1}{m_i \sigma^0 \sqrt{2\pi}} \cdot \exp\left[-\frac{(\ln(m_i) - \ln(\mu^0))^2}{2\sigma^{0^2}}\right]\ for\ t = 0$$

In Eq. 2, the first term on the left $\psi(m,t)$ represents the concentration density distribution of cell mass (m) at time (t), which is assumed spatially uniform. The second term is the cell growth term [21]. On the right hand side, the first term is multiplied by two as it represents the birth of two daughter cells from one mother cell, where m' refers to cells at division. The latter is consumed due to mitosis as represented by the second negative term. The last term represents the rate of cell death. In the above equation, the washout flux is not shown because a fed-batch bioreactor was used. All symbols are defined in the notations tables, shown as Table 1 and Table 2 in Section 3 of the paper. The growth rate for a single cell in the model is given by the following equation:

$$v(m, C_G) = \left(\frac{3}{d_C}\right)^{2/3} (4\pi)^{1/3} m^{2/3} \frac{\mu' C_G}{K_G + C_G} \frac{C_{L,O_2}}{C_m + C_{L,O_2}} - \mu_C m \quad (3)$$

This equation expresses cell mass change with time and it is obtained from the postulate of Bertalanffy 1932 and 1938 [27, 28]. The positive anabolic term is related to both glucose and oxygen and is considered in this model according to Michaelis-Menten and Monod kinetics. In contrast, the catabolic negative term is proportional to cell mass, indicating that the growth rate

decreases as cell mass increases. This is consistent with the hypothesis of cell growth ceasing after a maximum cell mass is reached.

Cell division rate, developed by Koch and Schaecter [29], describes how cell mass may be used as an estimator of cell division and is given by the following equation:

$$\Gamma^M(m, C_G) = v(m, C_G) \cdot \gamma^M(m) \tag{4}$$

where $\gamma^M(m) = \dfrac{f(m)}{1 - \int_0^m f(m')\,dm'}$ and $f(m) = \dfrac{1}{\sqrt{2\pi\sigma^2}} e^{\frac{-(m-\mu)^2}{2\sigma^2}}$.

Assuming that a cell divides when it reaches a critical mass, Γ^M is then deemed proportional to the growth rate and to the mass of the cell itself; it is expressed here as the distribution for cell division mass ($\gamma^M(m)$) [21]. $\gamma^M(m)$ normalizes the probability function of a cell of mass m to divide ($f(m)$), and is represented as a Gaussian distribution with mean μ and variance σ^2.

$$p(m, m') = \frac{1}{\beta(q, q)} \frac{1}{m'} \left(\frac{m}{m'}\right)^{q-1} \left(1 - \frac{m}{m'}\right)^{q-1} \tag{5}$$

$p(m,m')$ is identified as the partitioning function and describes how the cellular material is divided amongst the two daughter cells. It assumes that a symmetric division occurs, since this is the most probable outcome, even though the division may also be asymmetric. The peak of the probability function is centered at half the mother's cell size [30].

Numerous equations are used in the literature to model the death phase of cells. From a biological point of view, it is known that the probability of cell death increases with (a) increased cell age, (b) depletion of substrate concentration, and/or (c) accumulation of cell waste/by-products. In this model, a simplified form of Tremblay *et al.*'s equation [31] for cell death rate was used, and it is expressed by the following equation:

$$k_D = k_{Dmin} + (k_{Dmax} - k_{Dmin}) \frac{K_D}{K_D + C_G} \tag{6}$$

It is worthy to note that our model is also based on the assumption that cell death phase is initiated upon exhaustion of both dissolved O_2 and substrate concentrations, while the stationary phase begins when one of either the dissolved O_2 or substrate concentrations are equal to zero.

2.2 Gas and liquid phase balances

The concentration of glucose in the medium is given by the following mass balance equation:

$$\frac{dC_G}{dt} = F_L G_r - \frac{1}{Y_{B/G}}\frac{dN}{dt} \tag{7}$$

with $F_L = \frac{dV}{dt} = 0$ in batch culture and $\frac{dN}{dt} = \frac{N(ln(N) - ln(N_0))}{t}$.

Considering that in this bioreactor there is a liquid inflow without any outflow, the liquid phase balances for O_2, CO_2, N_2 and bicarbonate, used to find their concentrations, can be written by rearranging the equations from de Jonge *et al.*'s work [18]:

$$\frac{dC_{L,O_2}}{dt} = \frac{F_{Lin}}{V_{L0}} C_{L0,O_2} + k_L a_{B,O_2}\left(\frac{Px_{GB,O_2}}{RTm_{O_2}} - C_{L,O_2}\right) + k_L a_{H,O_2}\left(\frac{Px_{GH,O_2}}{RTm_{O_2}} - C_{L,O_2}\right) - OUR \tag{8}$$

$$\frac{dC_{L,CO_2}}{dt} = \frac{F_{Lin}}{V_{L0}} C_{L0,CO_2} + k_L a_{B,CO_2}\left(\frac{Px_{GB,CO_2}}{RTm_{CO_2}} - C_{L,CO_2}\right) + k_L a_{H,CO_2}\left(\frac{Px_{GH,CO_2}}{RTm_{CO_2}} - C_{L,CO_2}\right) + CEI - (k_{1f} + k_{2f}10^{pH-14})C_{L,CO_2} + (k_{2r} + k_{1r}10^{-pH})C_{L,HCO_3^-} \tag{9}$$

$$\frac{dC_{L,N_2}}{dt} = \frac{F_{Lin}}{V_{L0}} C_{L0,N_2} + k_L a_{B,N_2}\left(\frac{Px_{GB,N_2}}{RTm_{N_2}} - C_{L,N_2}\right) + k_L a_{H,N_2}\left(\frac{Px_{GH,N_2}}{RTm_{N_2}} - C_{L,N_2}\right) \tag{10}$$

$$\frac{dC_{L,HCO_3^-}}{dt} = \frac{F_{Lin}}{V_{L0}} C_{L0,HCO_3^-} + (k_{1f} + k_{2f}10^{pH-14})C_{L,CO_2} - (k_{2r} + k_{1r}10^{-pH})C_{L,HCO_3^-} \tag{11}$$

where the Oxygen Uptake Rate (OUR) is given by the following equation:

$$OUR = Y_{OXYGEN}\left(\frac{3}{d_C}\right)^{2/3}(4\pi)^{1/3}\mu_0'\frac{C_{L,O_2}}{C_m + C_{L,O_2}}\int_0^\infty m^{2/3}\psi dm + \mu_m\int_0^\infty m\psi dm \tag{12}$$

The first term on the right hand side represents the oxygen consumed by the cell for growth, while the second term represents the basic oxygen requirement for cell survival and maintenance.

The Carbon Dioxide Evolution Rate (CER) is given by the following equation:

$$CER = \alpha_1 \frac{dN}{dt} + \alpha_2 N + \alpha_3 \tag{13}$$

In this work, CO_2 evolution is assumed to be due to growth, maintenance requirements, and subproduct biosynthesis [32].

k_{1f}, k_{2f}, k_{1r}, k_{2r} are the reaction rate constants of the following reactions:

$$CO_2 + 2H_2O \underset{k_{1r}}{\overset{k_{1f}}{\rightleftharpoons}} HCO_3^- + H_3O^+ \tag{14}$$

$$CO_2 + OH^- \underset{k_{2r}}{\overset{k_{2f}}{\rightleftharpoons}} HCO_3^- \tag{15}$$

Mass transfer coefficients for dissolved $\mathbf{O_2}$ (k_La_{O2}) are largely determined empirically. In our model, the correlation for oxygen mass transfer (k_La_{O2}) was derived from the work done by Nikakhtari and Hill [33] and is expressed by the following equation:

$$k_L a_{O_2} = A_0 (N)^{A_1} (F_{G0})^{A_2} \tag{16}$$

Where N is the stirring speed (100 rpm), F_{G0} is the aeration rate and A_0, A_1, A_2 are three constants with the values 5.76×10^{-3}, 1.48, 0.253, respectively.

k_La_k, $k_La_{B,i}$, $k_La_{H,i}$ are the overall, bubbles-broth, and headspace-broth volumetric mass transfer coefficients, respectively, and they are given by the following equations:

$$k_L a_k = k_L a_{O_2} \sqrt{\frac{D_k}{D_{O_2}}} \qquad k = CO_2, N_2 \tag{17}$$

$$k_L a_{B,i} = \alpha k_L a_i \qquad 0 \le \alpha \le 1 \qquad i = O_2, CO_2, N_2 \tag{18}$$

$$k_L a_{H,i} = (1-\alpha) k_L a_i \qquad 0 \le \alpha \le 1 \qquad i = O_2, CO_2, N_2 \tag{19}$$

In order to accurately attain the concentrations of the gases (O_2, CO_2, N_2) in the liquid phase it is necessary first identify the mole fractions of O_2, CO_2 and N_2 in the gas bubbles (x_{GB}) and in the headspace (x_{GH}). These can be described by the following mass balance equations:

$$\frac{dx_{GB,i}}{dt} = \frac{F_{G0}}{V_{GB}} x_{G0,i} - \frac{F_{G1}}{V_{GB}} x_{GB,i} - k_L a_{B,i} \frac{V_L}{V_{GB}} \left(\frac{x_{GB,i}}{m_i} - c_{L,i} \frac{RT}{P} \right) \qquad i = O_2, CO_2, N_2 \tag{20}$$

$$\frac{dx_{GH,i}}{dt} = \frac{F_{G1}}{V_{GH}} x_{GB,i} - \frac{F_{G2}}{V_{GH}} x_{GH,i} - k_L a_{H,i} \frac{V_L}{V_{GH}} \left(\frac{x_{GH,i}}{m_i} - c_{L,i} \frac{RT}{P} \right) \qquad i = O_2, CO_2, N_2 \tag{21}$$

Where F_{G0} is the inlet gas flow, F_{G1} and F_{G2} are the gas flows from the broth to the headspace and from the headspace to the sensors, respectively, and are given by the following equations:

$$F_{G1} = \frac{F_{G0} - \sum_i k_L a_{B,i} V_L((x_{GB,i}/m_i) - c_{L,i}(RT/P))}{1 - (P_w/P)} \qquad i = O_2, CO_2, N_2 \qquad (22)$$

$$F_{G2} = \frac{(1 - (P_w/P))F_{G1} - \sum_i k_L a_{H,i} V_L((x_{GH,i}/m_i) - c_{L,i}(RT/P))}{1 - (P_w/P)} \qquad i = O_2, CO_2, N_2 \qquad (23)$$

All symbols are defined in the notations tables (Tables 1 and 2 in Section 3).

3. Model parameters and validation

The main objective of developing the model is to help understand the stem cell population growth behavior, and to then use this understanding to maximize the number of cells in the shortest possible time. The model is tested to assess its validity by showing that the modeled behaviors of O_2, CO_2, substrate concentration, and cell concentrations are comparable to those from literature data. In addition, it was possible to observe the three main phases of cell growth mentioned above.

Subsequently, simulations were conducted using the model starting with an initial volume of 100 ml over 250 hours. The modelling and simulations were implemented and solved in gPROMS (Process Systems Enterprise, UK).

Parameter values shown in the following table were extracted from the literature. The values of some parameters were adjusted to suit the units of measurement used in our model to maintain consistency.

Table 1 – Definitions and values (where applicable) of stem cell model parameters. Parameters marked with * are those used to fit the model to the literature experimental data.

Parameters	Description	Value	Unit	Reference
α	Mass transfer function	0.974	-	[18]
α_1	Constant relating CO_2 to growth	1.43×10^{-9}	mmol/cells	[32]
α_2	Constant relating CO_2 to maintenance energy	4×10^{-8}	mmol/(cells h)	[32]
α_3	Constant relating CO_2 to	1×10^{-10}	mmol/(mm^3 h)	[32]

	subproducts production			
β	Beta distribution	4.65×10^{-25}	-	[34]
γ^M	Distribution for cell division mass	-	1/g	-
Γ^M	Cell division rate	-	1/h	-
μ	Mean for division rate	3.8	ng	[34]
μ_c	Catabolic rate	1×10^{-3}	1/h	[34]
* μ_m	Rate of oxygen consumption for cell maintenance	1.61×10^{-11}	mmol/(ng*h)	[35]
μ'	Maximum specific growth rate	1.6×10^{3}	ng/(mm^2 h)	[35]
ψ	The number concentration density cell mass	-	cells/(ng $mm^{3)}$	-
σ	Standard deviation for division rate	1.125	ng	[34]
σ^0	standard deviation of the initial cell mass distribution	0.4	ng	[34]
μ^0	mean value of initial cell mass distribution	2	ng	[34]
* C_m	Oxygen concentration at half maximum consumption	0.06×10^{-7}	mmol/mm^3	[35]
d_c	Cell density	1.14×10^{6}	ng/mm^3	[36]
D_{CO2}	CO_2 diffusion coefficient	1.92×10^{-9}	m^2/s	[18]
D_{N2}	N_2 diffusion coefficient	2.30×10^{-9}	m^2/s	[18]
D_{O2}	O_2 diffusion coefficient	2.32×10^{-9}	m^2/s	[18]
f(m)	Probability distribution for the transition rate to mitosis	-	1/g	-
F_{g0}	Initial gas flow	Different for each simulation	ml/h	This work
F_L	Liquid flow	Different for each simulation	mm^3/h	This work
k_{1f}	Forward reaction rate constant	1.29×10^{2}	1/h	[18]

k_{2f}	Forward reaction rate constant	8.55×10^{-14}	$mm^3/(mmol\ h)$	[18]
k_{1r}	Backward reaction rate constant	1.81×10^{11}	$mm^3/(mmol\ h)$	[18]
k_{2r}	Backward reaction rate constant	1.44	1/h	[18]
k_{dmin}	Minimum specific death rate	0.0	1/h	[37]
* k_{dmax}	Maximum specific death rate	1.16×10^{-3}	1/h	[37]
* K_D	Constant for specific death rate	9.75×10^{-2}	g/l	[37]
* K_G	Glucose Monod constant	0.09	g/l	[37]
m_{max}	Maximum cell mass	16	ng	[37]
m_{CO2}	CO_2 partition coefficient	1.17	-	[18]
m_{N2}	N_2 partition coefficient	65.87	-	[18]
m_{O2}	O_2 partition coefficient	33.31	-	[18]
N	Cell number distribution	-	$cells/mm^3$	-
N_0	Initial cell number distribution	10×10^4	$Cells/mm^3$	[34]
P	Total pressure in the bioreactor	1.3×10^5	Pa	[18]
P_w	Water vapor pressure	3.2×10^3	Pa	[18]
q	Partition factor	40	-	[34]
T	Temperature in the reactor	310.15	K	This work
v	Growth rate of the cell	-	g/l	-
V_{GB}	Gas bubbles phase volume	9.88×10^3	mm^3	This work
V_{GH}	Gas headspace volume	63.25×10^3	mm^3	This work
V_{L0}	Initial liquid volume	100×10^3	mm^3	This work
* $Y_{B/G}$	Yield of number of cells per gram of glucose	4.95×10^5	cell/(g gluc)	[37]
* Y_{OXYGEN}	Yield of number of cells per mole of oxygen	0.56×10^{-9}	mmol/ng	[37]
* Y_{OXYGEN} μ_0,	-	0.903×10^{-8}	$mmol/(mm^2\ h)$	[35]

Table 2 - Measured variables with their initial conditions.

Measured Variables	Description	Initial Condition	Unit	Reference
C_{LCO2}	CO_2 concentration	0	$mmol/mm^3$	This work
C_{LO2}	O_2 concentration	Different for each simulation	$mmol/mm^3$	This work
C_{LN2}	N_2 concentration	0	$mmol/mm^3$	This work
C_{LHCO3}	HCO_3^- concentration	0.0001	$mmol/mm^3$	This work
C_G	Glucose concentration	Different for each simulation	g/l	This work
x_{GBCO2}	CO_2 mole fraction related to gas bubble phase	0.00045	-	[18]
x_{GBO2}	O_2 mole fraction related to gas bubble phase	0.20950	-	[18]
x_{GBN2}	N_2 mole fraction related to gas bubble phase	0.79005	-	[18]

Before the model can be used to formulate predictions about the effects of certain variables and inputs on cell proliferation, it must first be validated. The model has been tested by comparison with literature data taken from the dissertation by Sen [38]. The fit between our model's prediction and Sen's literature data is shown in Figure 3. The parameters marked with * in Table 1 were estimated in order to fit the model against the literature data and the fit can be considered decent in representing our model in terms of tracking the overall trend of the experimental cell population behaviour. The comparison was limited to cell concentration due to the lack of experimental data and the difficulty in finding compatible data from literature.

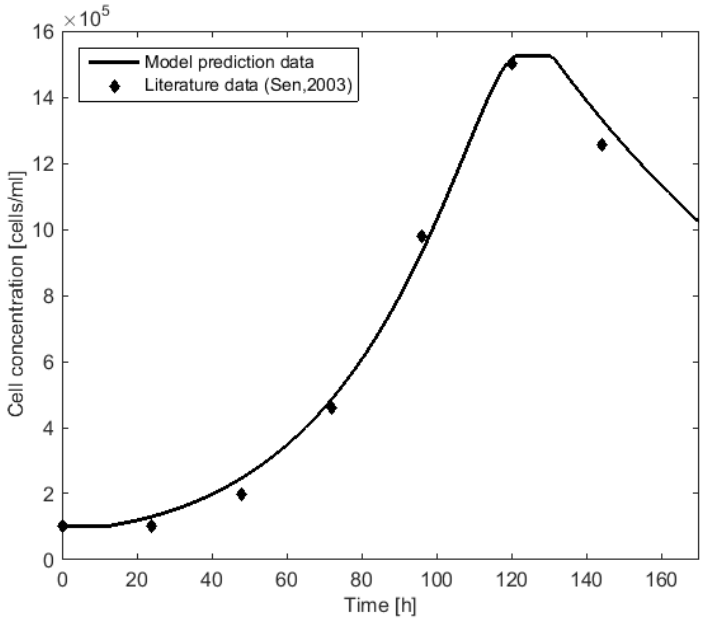

Figure 3 - Comparison of the model prediction of stem cell concentration with literature data from Sen [38].

4. Model simulation analysis

4.1 Varying initial substrate (glucose) concentration in batch mode

The first simulation for a bioreactor in batch mode was conducted to analyze the effect of changing the initial concentration of glucose on cell growth and oxygen consumption. Three different initial concentrations were used: 1.5 g/l, 3 g/l, and 5 g/l. A higher initial substrate concentration resulted in an increase in both the time required for glucose depletion (Figure 4 - A) and the total cell number (Figure 4 - C). It should however be noted that the decrease of the stationary phase caused by the increase of the initial concentration of glucose is due to the augmentation of cell number. A greater number of cells results in faster oxygen consumption (Figure 4 - B), leading to an earlier onset of the death phase.

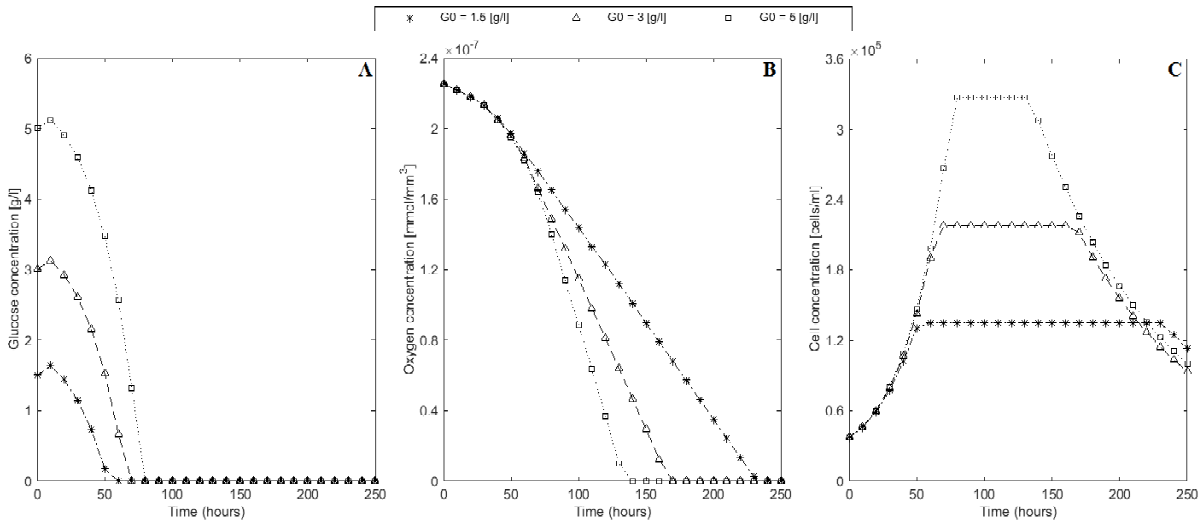

Figure 4 - Glucose depletion (A), oxygen depletion (B), and cell concentration (C) over time at three varying starting concentrations of glucose (1.5, 3, and 5 g/l). Glucose diminishes at a faster rate with a decrease in initial glucose concentration. Oxygen consumption is accelerated with an increase in the initial glucose concentration [$O_0 = 0.225 \times 10^{-6}$ (mmol/mm^3)]. With an increase in initial glucose concentration, there is an increase in cell number (N_0= 37500).

4.2 Carbon dioxide control in batch mode

The CO_2 level in the bioreactor is also an imperative variable that should ideally be controlled and was thus included in our model. The parameters (α_1, α_2, α_3) in the CER equation (Eq. 13) were adopted from the data obtained by Birol *et al.* [32]. The effect of varying the initial glucose concentration on CO_2 concentration is displayed in Figure 5. The observed suggests, as expected, that an increase in initial substrate concentration brought about increased levels of CO_2. Also, there is an evident upward shift in both the growing and exponential phases and a downward shift in the death phase (Figure 5).

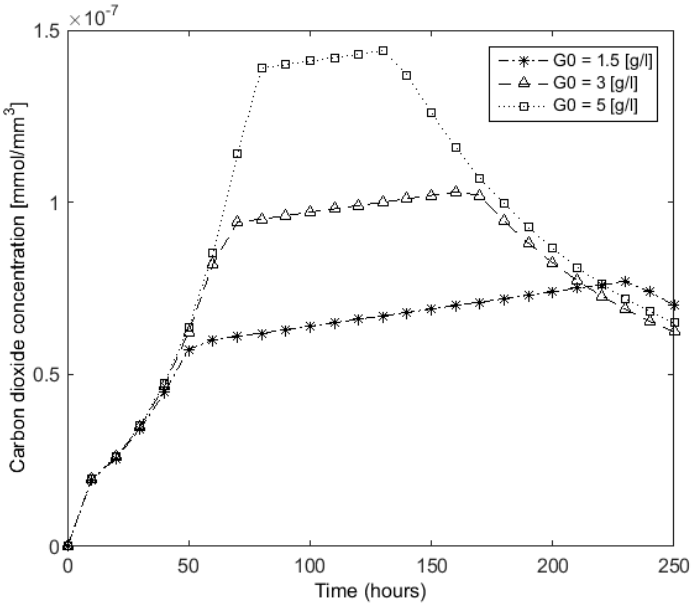

Figure 5 - CO_2 concentration over time at three varying starting concentrations of glucose (1.5, 3, and 5 g/l).

4.3 Varying initial conditions of oxygen in batch mode

Similar simulations were conducted by varying the initial concentration of O_2. Three different oxygen conditions were simulated:

- Hypoxic – 5% O_2 (0.05×10^{-6} mmol/mm^3)
- Normoxic – 21% O_2 (0.225×10^{-6} mmol/mm^3)
- Hyperoxic – 35% O_2 (0.38×10^{-6} mmol/mm^3)

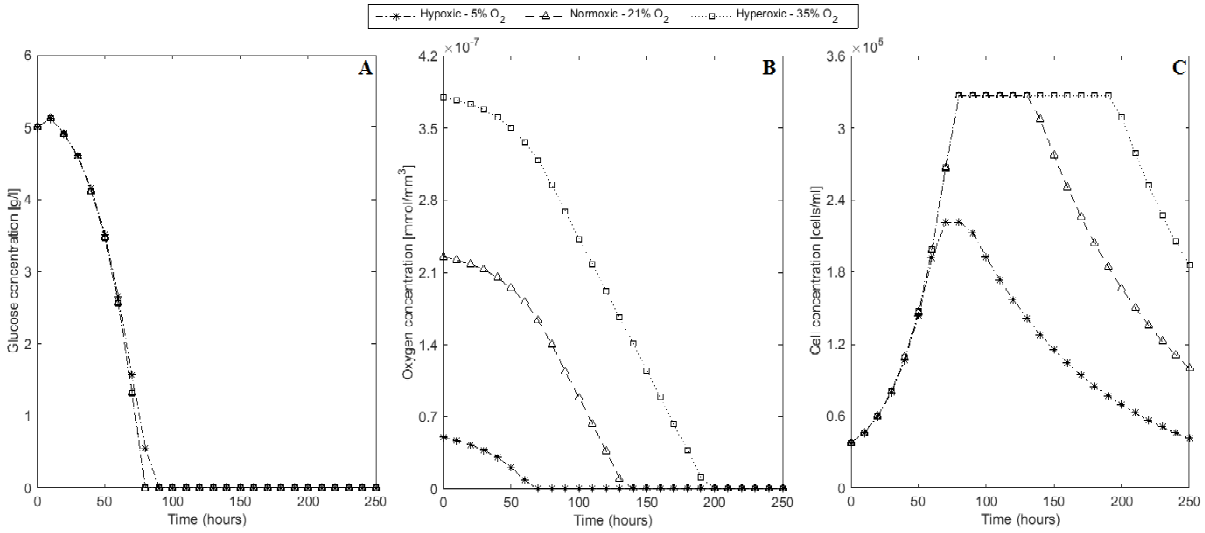

Figure 6 - Glucose depletion (A), Oxygen depletion (B), and cell concentration (C) over time at three varying starting concentrations of dissolved O_2 (5, 21, and 35 %).

Hyperoxia resulted in a decrease in the rate of O_2 depletion (Figure 6 - B) and thus an increase in the rate of glucose depletion (Figure 6 - A) and a prolongation of the stationary phase of cells (Figure 6 - C). Although hypoxia caused downward shift in the cell growth, there is no apparent difference in cell growth between normoxic and hyperoxic culture conditions, other than the extension of the stationary phase (Figure 6 - C). Cells in the hypoxic conditions stop proliferating at an earlier stage during the culture period due to the more rapid exhaustion of oxygen with time.

The O_2 tension stimulates stem cell growth by varying the production of growth factors, surface markers, transcription factors and by also obstructing cellular respiratory pathways [39]. From the literature, it can be concluded that hypoxic conditions (2-5 % O_2) are broadly preferred to retain stem cell pluripotency, while normoxic conditions (20 % O_2) improve the growth and expansion of mature cells [40].

4.4 Varying inoculum concentration in batch mode

A sensitivity analysis was carried out on the starting inoculum concentration of cells in order to determine its effect on the final cell population and on the substrate concentration profiles. For the following simulation results, the only parameter altered was the initial cell concentration.

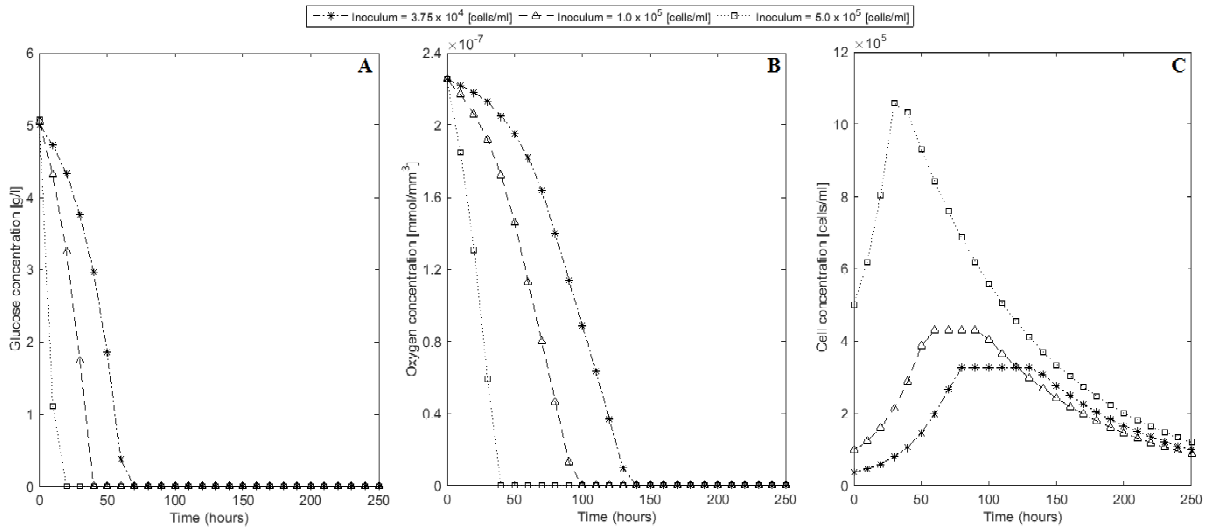

Figure 7 - Glucose depletion [G_0 = 5 (g/l)] (**A**), Oxygen depletion [$O_0 = 2.25 \times 10^{-5}$ (mmol/mm^3)] (**B**), and cell concentration (**C**) over time at three varying starting cell inoculum concentrations (3.75×10^4, 1.0×10^5, and 5.0×10^5 cells/ml).

Figure 7 illustrates the effect of varying the starting cell inoculum concentrations on various parameters. With an increase in inoculum concentration, there is an increase in the rate of both glucose and oxygen depletion (Figures 7 - A and B) and an increase in the overall cell number and growth rates (Figure 7 - C). Moreover, higher inoculum density brought about a left-shift to the cell growth curve and hence a faster onset of the stationary phase (Figure 7 - C). It can therefore be deduced that the increased growth rates lead to increased rate of substrate consumption, and hence earlier onset of the stationary phase. Furthermore, for at all inoculum values plotted, the concentrations of both substrates (glucose and O_2) were found to decrease to zero, resulting in the onset of the death phase. Parallel with the other simulations, the onset of the death phase was assumed to coincide with the reduction of both substrate concentrations to zero.

4.5 Varying medium inflow in fed-batch mode

All above simulations have been carried out assuming a batch bioreactor. In the following simulations, a fed-batch bioreactor will be assumed instead, while also introducing a medium inflow and an inlet gas flow.

The effect of feed flow-rate into the bioreactor was analyzed by carrying out simulations with varying feed-flows. The initial volume of the medium was assumed to be 100 ml, and the maximum 500 ml. The feed flow-rates for which simulations were conducted are 10, 50, and 100 ml/h.

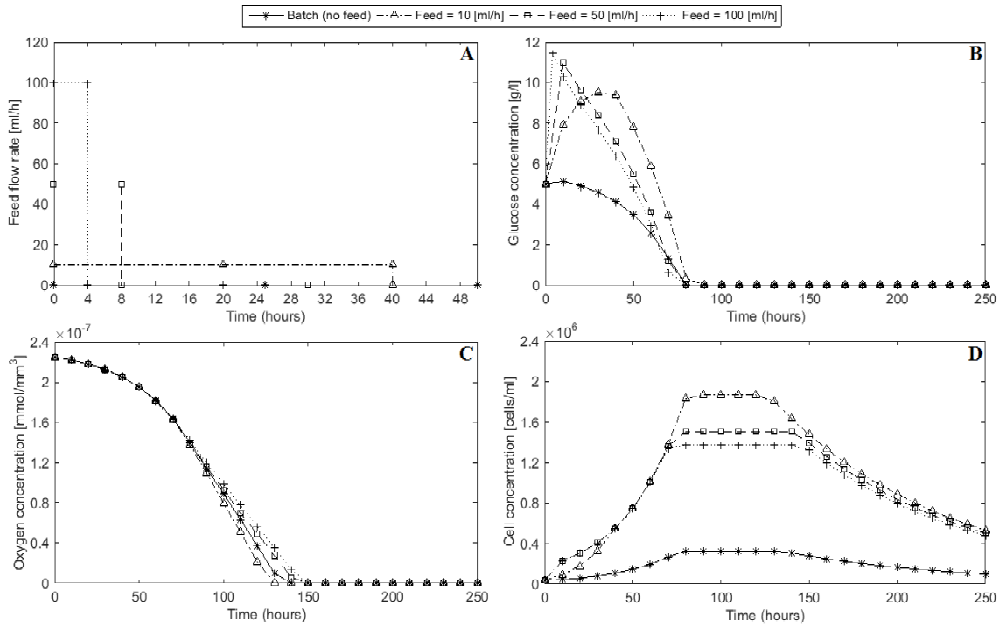

Figure 8 - Feed flow rate (A), glucose consumption [G_0 = 5 (g/l)] (B), oxygen consumption [O_0 = 0.225 × 10^{-6} (mmol/mm^3)] (C), and cell concentration (N_0= 37500) (D) over time with varying medium inflow (10, 50, and 100 ml/h) versus batch bioreactor (no medium inflow).

From Figure 8, it can firstly be deduced that in batch systems, glucose depletion rate is increased (Figure 8 - B) and cell concentrations are significantly decreased (Figure 8 - D). Generally, average glucose consumption rate is constant over time; however, in fed-batch systems, glucose concentrations rapidly increase and then rapidly decrease again in a constant manner. Also, maximum cell concentration is independent of feed flow-rate. This can be justified by the overall volume being larger at higher feed flow rates and hence cell concentrations are more dilute. This is parallel to the feed flow-rate profiles (Figure 8 - A), for the bioreactor cannot have infinite volume; instead we have allocated a maximum volume of 500 ml. And clearly, the faster the flow-rate, the quicker the maximum volume is reached: the time required to reach the maximum volume of 500 ml is 4, 8, and 40 hours for a flow-rate of 100, 50, and 10 ml/h, respectively. This considerable

difference in time also leads to different feeding times, reaching a gap of 36 hours between the highest and the lowest feed flow-rate.

Sharp increases in cell concentration can be observed in the early stages of the simulation due to the sudden increases in glucose concentration via increases in feed flow-rate. These observations coincide with the glucose concentration profiles in Figure 8 - B, where higher feed flow-rates bring about sharper increases in glucose concentrations early on in the simulation.

This model is based on the assumption that the stationary phase initiates when one of the substrates reaches zero. From the glucose equation, it can be inferred that the feed term ($F_L G_r$) is dependent on the feeding time. If the feed flow-rate (F_L) reaches zero early, leaving only the consumption term $\frac{dC_G}{dt} = -\frac{1}{Y_{B/G}}\frac{dN}{dt}$ within the equation, it is clear that the glucose will be consumed first. Despite the larger values for maximum glucose concentration under higher flow-rates scenarios, these are counteracted by a larger glucose consumption term, leading to an earlier onset of the stationary phase. Therefore, in order to obtain the value of the maximum cell concentration, it is important to optimize the feed flow-rate and obtain the optimal value that yields enhanced cell growth.

4.6 Varying inlet gas flow in fed-batch mode

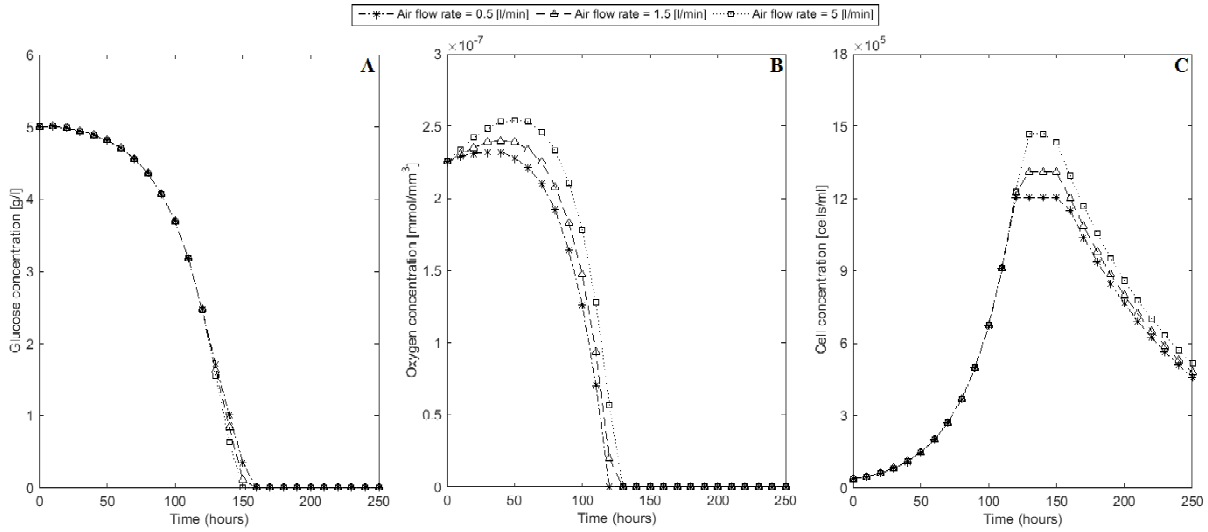

Figure 9 - Glucose consumption [G_0 = 5 (g/l)] (A), oxygen consumption [O_0 = 0.225 × 10^{-6} (mmol/mm^3)] (B), and cell concentration (N_0= 37500) (C) over time with varying inlet gas flow-rates (0.5, 1.5, and 5 l/min).

From Figure 9 - C it is evident that increased air flow-rates shift cell concentration curves upwards. These findings are parallel to results in Figure 9 - B which illustrate that with an increase in gas flow-rate, there is a subsequent prolongation in the presence of oxygen, and thus an increase in the time the cells spend in the stationary phase.

5. Conclusion

In this work, we have developed a population balance model that successfully simulates the proliferation of stem cells. The model parameters were presented and model validated against limited available literature data. Simulation results corroborated literature findings.

From the simulation studies, it was shown that attaining the objective of maximum cell concentrations in the shortest time requires increasing initial concentrations of the glucose and O2, using a fed-batch bioreactor system with a low substrate feeding rate, incremental increase in inflow rate of the O2, and, initiating the cell proliferation with an inoculum of high density, therefore aiding in the design of optimisation and control systems for this complex process.

The model is limited in that the relationship between the concentration of CO_2 and the death kinetics was not explicitly made, and the model does not consider the effects of multiple metabolites such as glutamine, lactate, or ammonia. It would be possible to improve on the kinetics through the use of dual Michaelis-Menten kinetics [41] which take into consideration the presence of glucose. This work provides a proof-of-concept of a cell-level model describing stem cell culture in 3D bioreactors, and paves the way forward for parameter estimation using experimental data as well as for dynamic optimization studies that identify .

Acknowledgements

This work was funded in part by a research fellowship from the Harvard Club of Australia Foundation (AA).

References

1. ASCC, Fact Sheet 1 - What are Stem Cells? CENTRE, A. S. C., 2010.

2. Bauwens, C., et al., Development of a perfusion fed bioreactor for embryonic stem cell-derived cardiomyocyte generation: Oxygen-mediated enhancement of cardiomyocyte output. Biotechnology and Bioengineering, 2005. **90**(4): p. 452-461.
3. Boheler, K.R., et al., Differentiation of pluripotent embryonic stem cells into cardiomyocytes. Circulation Research, 2002. **91**(3): p. 189-201.
4. Penn, M.S. and K.H. Silver, Strategies for cardiovascular repair: role of stem cells in 2012 and beyond. Minerva Cardioangiologica, 2012. **60**(5).
5. Gomez-Barrena, E., et al., Bone regeneration: stem cell therapies and clinical studies in orthopaedics and traumatology. Journal of Cellular and Molecular Medicine, 2011. **15**(6).
6. Becker, S., Recent Advances towards the Clinical Application of stem cells for Retinal Regeneration. Cells, 2012. **1**.
7. Lescaudron, L., et al., The Use of Stem Cells in Regenerative Medicine for Parkinson's and Huntington's Diseases. Current Medicinal Chemistry, 2012. **19**(35).
8. Fiorina, P., et al., Immunological Applications of Stem Cells in Type 1 Diabetes. Endocrine Reviews, 2011. **32**(6).
9. Maltais, S., et al., Stem cell therapy for chronic heart failure: an updated appraisal Expert Opinion on Biological Therapy, 2013. **13**(4).
10. Rodrigues, C.A.V., et al., Stem cell cultivation in bioreactors. Biotechnology Advances, 2011. **29**(6): p. 815-829.
11. Julian Chaudhuri and M. Al-Rubeai, Bioreactors for Tissue Engineering: Principles, Design and Operation2005: Springer.
12. King, J.A. and W.M. Miller, Bioreactor development for stem cell expansion and controlled differentiation. Current Opinion in Chemical Biology, 2007. **11**(4): p. 394-398.
13. Storm, M.P., et al., Three-dimensional culture systems for the expansion of pluripotent embryonic stem cells. Biotechnology and Bioengineering, 2010. **107**(4): p. 683-695.
14. Thomson, H., Bioprocessing of embryonic stem cells for drug discovery. Trends in Biotechnology, 2007. **25**(5): p. 224-230.
15. Ramkrishna, D., Population balances: Theory and applications to particulate systems in engineering2000: Academic press.
16. Garcia-Ochoa, F. and E. Gomez, Bioreactor scale-up and oxygen transfer rate in microbial processes: an overview. Biotechnology Advances, 2009. **27**(2): p. 153-176.
17. Pörtner, R. and T. Schäfer, Modelling hybridoma cell growth and metabolism—a comparison of selected models and data. Journal of Biotechnology, 1996. **49**(1): p. 119-135.
18. de Jonge, L.P., J.J. Heijnen, and W.M. van Gulik, Reconstruction of the oxygen uptake and carbon dioxide evolution rates of microbial cultures at near-neutral pH during highly dynamic conditions. Biochemical Engineering Journal, 2014. **83**: p. 42-54.
19. Parolini, D.N. and S. Carcano, A model for cell growth in batch bioreactors. 2010.
20. Eakman, J.M., Models for the dynamics and statistics of microbial populations, 1966, Univ. of Minnesota. p. 180 l.
21. Mancuso, L., et al., Experimental analysis and modelling of in vitro proliferation of mesenchymal stem cells. Cell Prolif, 2009. **42**(5).
22. Mancuso, L., et al., Experimental analysis and modeling of bone marrow mesenchymal stem cells proliferation. Chemical Engineering Science, 2010. **65**(1).
23. Fredrickson, A.G., D. Ramkrishna, and H.M. Tsuchiya, Statistics and dynamics of procaryotic cell populations. Mathematical Biosciences, 1967. **1**(3): p. 327-374.
24. Hjortsø, M.A., Population Balances in Biomedical Engineering: Segregation Through the Distribution of Cell States2005: McGraw-Hill.
25. Hatzis, C., F. Srienc, and A.G. Fredrickson, Multistaged corpuscular models of microbial growth: Monte Carlo simulations. Biosystems, 1995. **36**(1): p. 19-35.

26. Mantzaris, N.V., et al., Numerical solution of a mass structured cell population balance model in an environment of changing substrate concentration. Journal of Biotechnology, 1999. **71**(1-3): p. 157-174.
27. Von Bertalanffy, L., Theoretische biologie. Vol. 1. 1932: Gebrüder Borntraeger.
28. Bertalanffy, L.v., A quantitative theory of organic growth. Hum. BioI. 10 (2): 181, 1938. **213**.
29. Koch, A. and M. Schaechter, A model for statistics of the cell division process. Journal of General Microbiology, 1962. **29**(3): p. 435-454.
30. Hatzis, C., F. Srienc, and A. Fredrickson, Multistaged corpuscular models of microbial growth: Monte Carlo simulations. Biosystems, 1995. **36**(1): p. 19-35.
31. De Tremblay, M., et al., Optimization of fed-batch culture of hybridoma cells using dynamic programming: single and multi feed cases. Bioprocess Engineering, 1992. **7**(5): p. 229-234.
32. Birol, G., C. Ündey, and A. Cinar, A modular simulation package for fed-batch fermentation: penicillin production. Computers & Chemical Engineering, 2002. **26**(11): p. 1553-1565.
33. Nikakhtari, H. and G.A. Hill, Modelling Oxygen Transfer and Aerobic Growth in Shake Flasks and Well-Mixed Bioreactors. The Canadian Journal of Chemical Engineering, 2005. **83**(3): p. 493-499.
34. Manoli, H., A Validated Model of Stem Cells in 3D Suspension, 2012, University of Sydney.
35. Pisu, M., et al., Modeling of engineered cartilage growth in rotating bioreactors. Chemical Engineering Science, 2004. **59**(22-23).
36. Jakob, M., et al., Enzymatic digestion of adult human articular cartilage yields a small fraction of the total available cells. Connective tissue research, 2003. **44**(3-4): p. 173-180.
37. Costamagna, E., Modelling of Hematopoietic Stem Cells for Autologous transplantation Leukemia theraphy expansion in Bioreactors, 2013-2014, Politecnico di Torino.
38. Sen, A., Bioreactor protocols for the long-term expansion of mammalian neural stem cells in suspension culture. 2003.
39. Lim, M., Ye, H., Panoskaltsis, N., Drakakis, E. M., Yue, X., Cass, A. E., Radomska, A., Mantalaris, A. , Intelligent bioprocessing for haemotopoietic cell cultures using monitoring and design of experiments. Biotechnol Adv., 2007. **25**.
40. Guitart, A.V., Hammoud, M., Dello Sbarba, P., Ivanovic, Z., Praloran, V., Slow-cycling/quiescence balance of hematopoietic stem cells is related to physiological gradient of oxygen. Exp Hematol, 2010. **38**.
41. Davidson, E.A., et al., The Dual Arrhenius and Michaelis–Menten kinetics model for decomposition of soil organic matter at hourly to seasonal time scales. Global Change Biology, 2012. **18**(1): p. 371-384.
42. Hamad M., Manoli H., Irhimeh M., Khademhosseini A., Abbas A., (2014), Population balance modelling of stem cell culture in 3D suspension bioreactors, Chemeca 2014, Perth, Australia, 28 Sep – 1 Oct.